

# Unusual X-ray transients in the Galactic Centre

M. Sakano<sup>1</sup>, R. S. Warwick<sup>1</sup>, A. Decourchelle<sup>2</sup> and Q. D. Wang<sup>3</sup>

<sup>1</sup>*Department of Physics and Astronomy, University of Leicester, Leicester LE1 7RH, UK*

<sup>2</sup>*CEA/DSM/DAPNIA, Service d'Astrophysique, C.E. Saclay, 91191 Gif-sur-Yvette Cedex, France*

<sup>3</sup>*Astronomy Department, University of Massachusetts, Amherst, USA*

Accepted XXXX. Received XXXX 2003

## ABSTRACT

We report the discovery in the Galactic Centre region of two hard X-ray sources, designated as XMM J174457–2850.3 and XMM J174544–2913.0, which exhibited flux variations in the 2–10 keV band in excess of a factor of 100 in observations spanning roughly a year. In both cases the observed hydrogen column density is consistent with a location near to the Galactic Centre, implying peak X-ray luminosities of  $\sim 5 \times 10^{34}$  erg s<sup>-1</sup>. These objects may represent a new population of transient source with very different properties to the much more luminous Galactic Centre transients associated with neutron star and black-hole binary systems. Spectral analysis shows that XMM J174457–2850.3 has relatively weak iron-line emission set against a very hard continuum. XMM J174544–2913.0, on the other hand, has an extremely strong K-line from helium-like iron with an equivalent width of  $\sim 2.4$  keV. The nature of the latter source is of particular interest. Does it represent an entirely new class of object or does it correspond to a known class of source in a very extreme configuration?

**Key words:** Galaxy:centre – X-rays:binaries – X-rays:individual:XMM J174457–2850.3 – X-rays:individual:XMM J174544–2913.0

## 1 INTRODUCTION

During the last four years, the Galactic Centre region has been observed repeatedly by *Chandra* and *XMM-Newton*, including several extensive campaigns focused on Sgr A\* (e.g., Baganoff et al. 2001, 2003; Goldwurm et al. 2003; Porquet et al. 2003). Both observatories have also carried out wide-angle X-ray surveys in which sets of overlapping pointings have been used to give coverage of the Galactic plane within 1° of the Galactic Centre (Wang, Gotthelf & Lang 2002; Warwick 2002; Sakano et al. 2004c). The excellent imaging capability and high sensitivity of the two observatories has allowed the discrete X-ray source population in the direction of the Galactic Centre to be studied over a range in X-ray luminosity extending from 10<sup>38</sup> erg s<sup>-1</sup> down to  $\sim 10^{31}$  erg s<sup>-1</sup>. The temporal and spectral properties of Galactic Centre low-mass and high-mass X-ray binaries, typically seen in outburst with  $L_X > 10^{36}$  erg s<sup>-1</sup>, are now well established through the work of numerous missions, past and present, including most recently *RXTE*. However, much less is known about Galactic Centre sources with peak luminosities below  $\sim 10^{35}$  erg s<sup>-1</sup>, since this is close to the effective detection limit for earlier hard X-ray imaging missions such as *ASCA* and *SAX*. In essence, the recent surveys of *Chandra* and *XMM-Newton* have provided a new window on faint

source populations at the Galactic Centre (e.g., Munro et al. 2003a, 2003b, 2004b).

The spectra of the X-ray sources in the Galactic Centre Region with  $L_X > 10^{35}$  erg s<sup>-1</sup>, most of which are low-mass X-ray binaries (LMXB) containing either a neutron star or black hole, are often featureless (Sidoli et al. 1999; Sakano et al. 2002). On the other hand, Wang et al. (2002) report that the summed spectrum of the faint sources detected in the *Chandra* wide-angle Galactic Centre Survey shows significant 6.7 keV Fe K-line emission, implying the existence of one or more different populations of sources at lower luminosity. More recently, the  $\sim 2000$  X-ray sources detected in the very deep *Chandra* observations of the field around Sgr A\*, have been shown on average to have very hard (photon index  $\Gamma < 1$ ) spectra in addition to strong He-like and H-like K-lines from Si, S, Ar, Ca and Fe (Munro et al. 2003a, 2004b). Although resolved point sources contribute up to  $\sim 10\%$  of total hard X-ray emission from the Galactic Centre, the bulk of the X-ray luminosity of the region must either be truly diffuse in nature or originate in a very faint population of point sources with very hard spectra which are more numerous than cataclysmic variables (Munro et al. 2003a, 2004a). In the case of the former, it remains unclear whether thermal or non-thermal process dominate and what is the energising source of the plasma.

Comparing Galactic Centre observations taken at dif-

arXiv:astro-ph/0412236v1 9 Dec 2004

ferent epochs it is straightforward to pick out highly variable or transient X-ray sources. In this paper we present the results for two such transient sources with peak observed luminosities of  $\sim 5 \times 10^{34}$  erg s $^{-1}$ , which have interesting spectral properties. We also comment on what contribution such sources, in relative quiescence, might make to the unresolved X-ray hard emission of the Galactic Centre.

## 2 OBSERVATIONS

We have searched for transient X-ray sources by comparing images from the wide-angle X-ray surveys of the Galactic Centre region carried out by *Chandra* and *XMM-Newton* (Wang et al. 2002; Warwick 2002; Sakano, Warwick & Decourchelle 2003). The results of a full analysis will be discussed in a later paper and here we confine our attention to two relatively bright transients with interesting spectral properties.

Fig. 1 shows a sub-region from the image mosaics produced from the *XMM-Newton* and *Chandra* Galactic Centre surveys. The locations of the two transient sources, designated as XMM J174457–2850.3 and XMM J174544–2913.0, are indicated. Both sources are relatively bright in the *XMM-Newton* map but not visible in the corresponding *Chandra* image. Based on the *XMM-Newton* data, their positions (RA, DEC, J2000) are determined to be (17<sup>h</sup> 44<sup>m</sup> 57<sup>s</sup>.34, –28° 50′ 20<sup>.</sup>3) and (17<sup>h</sup> 45<sup>m</sup> 44<sup>s</sup>.51, –29° 13′ 0<sup>.</sup>6), respectively, with an error radius of 4 arc-sec.

Having identified the two sources of interest, we focus on the individual *XMM-Newton* and *Chandra* observations which encompass their positions (see Table 1). In the case of *XMM-Newton*, the data are from the EPIC instrument, which consists of three cameras, two utilising MOS CCDs (Turner et al. 2001) and one employing a pn CCD (Strüder et al. 2001). In the present observations the EPIC MOS and pn cameras were operated in *Full Frame Mode* and *Extended Full Frame Mode*, respectively, with the medium filter selected. We have used the Standard Analysis Software (SAS) Version 5.3 for the data filtering and reduction. Observing periods affected by high levels of background flaring identified in the light curve of the full-field data above 10 keV were rejected. For the MOS cameras we utilised pixel patterns of 0–12 (single to quadruple), whereas for the pn camera, we accepted single and double (pattern 0–4) events. All the *Chandra*/ACIS observations were carried out in Faint mode, with the optical axis located at the nominal position of ACIS-I. The data reduction and filtering were performed with the *Chandra* Interactive Analysis Software (CIAO) Version 2.3. We used events with the single to quadruple pixel patterns. The *Chandra* observations targeted on Sgr A\* (Table 1), carried out from 22 May to 4 June, 2002 have essentially the same attitude and for the spectral and image analysis considered in §3.1 were treated as one dataset.

## 3 RESULTS

### 3.1 XMM J174457–2850.3

The location of XMM J174457–2850.3 lies within the field of view of 10 of the pointings listed in Table 1. Table 2

summarises, in chronological order, the various flux determinations at the source position. Here we quote  $3\sigma$  upper limits when the source was not detected and  $1\sigma$  errors on significant detections using the 2–8 keV band image.

This source is most clearly detected in the *XMM-Newton* GC6 observation carried out on 2001/9/04, while two months earlier and ten months later the source was found to be 40–400 times fainter (Table 2). Fig. 2 shows an image of the source region obtained from the combined 2002 *Chandra* data when the source was in a particularly low state. The overlaid contours represent the point spread function (PSF) at the position of a local peak which, within the errors, is coincident with the *XMM-Newton* position\*. There are low-surface brightness features to the south and east of this peak. Comparing the photon statistics of the peak and its surroundings, we estimate the significance of the point source in these observations to be  $7.4\sigma$ .

When the source was in its high state (GC6 observation: Table 2), there was evidence for low-amplitude temporal variations. For example a trial fitting of the light curve, with a constant emission model (after the background is subtracted), for a binning of 32 s, is rejected at more than 99.9% confidence via  $\chi^2$ -test. On the other hand no distinct burst, flare, or dip behaviour was apparent. Extracting a power density spectrum reveals a slight excess of power above the Poisson noise level at  $\sim 0.06$  Hz and at frequencies below  $\lesssim 0.005$  Hz. A search for pulsations using a fast Fourier transformation (FFT) algorithm showed evidence of a peak at  $\sim 0.19$  Hz. An epoch folding search gave the best-fitting period to be 5.2521 s with a nominal error ( $P^2/t$ ) of 0.0012 s. The folded light curve with this period shows a sinusoidal form with a maximum relative amplitude of 20%. However, given the relatively poor signal to noise ratio, the reliability of this putative periodic signal is very uncertain.

The spectrum of the source as recorded by the *XMM-Newton* MOS cameras in the GC6 observation was extracted using an elliptical region of semi-axis dimensions 52'' and 18'' centred on the source position and aligned with the PSF (*nb.* this cell shape and alignment was in part dictated by the position of the source at the edge of the MOS field of view). Corresponding background spectra were taken from a nearby sky region of the same shape and orientation as the source region, chosen so as to avoid the weak sources detected in the corresponding *Chandra* observations. The source was outside of the field of view of the EPIC pn camera.

Fig. 3 shows the *XMM* MOS1 and MOS2 spectra after background subtraction. The observed spectrum is relatively featureless except for a possible excess signal around 6–7 keV. We fitted the two MOS spectra simultaneously with a power-law component modified by interstellar absorption, and found that this simple model well approximated the data ( $\chi^2/\text{dof}=63.8/77$ ). Nevertheless, when a narrow Gaussian line was added in the 6–7 keV range the fit improved ( $\chi^2/\text{dof}=58.9/75$ ) with a significance of 95% as measured by

\* The local peak is detected at (RA, Dec) = (17<sup>h</sup> 44<sup>m</sup> 57<sup>s</sup>.3, –28° 50′ 26'') within an error radius of 10''; the large uncertainty in the position is due to the 13.6 arcmin offset from the optical axis.

**Table 1.** *XMM-Newton* and *Chandra* observations used in the present analysis.

Name	Obs-ID	RA (J2000)	DEC (J2000)	Obs. Date (yyyy/mm/dd)	Net Exp. <sup>a</sup> (ks)
<i>XMM-Newton</i>					
GC10	0112971001	17 <sup>h</sup> 46 <sup>m</sup> 40 <sup>s</sup>	−29° 13′ 00″	2000/09/24	9.5/9.5/7.8
GRO J1744−28	0112971901	17 <sup>h</sup> 44 <sup>m</sup> 34 <sup>s</sup>	−28° 45′ 22″	2001/04/01	8.7/8.9/4.1
GC6	0112972101	17 <sup>h</sup> 45 <sup>m</sup> 40 <sup>s</sup>	−29° 00′ 23″	2001/09/04	22.4/24.0/17.5
<i>Chandra</i>					
GCS 12	2279	17 <sup>h</sup> 45 <sup>m</sup> 19 <sup>s</sup>	−28° 40′ 22″	2001/07/18	11.6
GCS 14	2284	17 <sup>h</sup> 45 <sup>m</sup> 37 <sup>s</sup>	−28° 56′ 27″	2001/07/18	10.6
GCS 15	2287	17 <sup>h</sup> 44 <sup>m</sup> 51 <sup>s</sup>	−28° 50′ 21″	2001/07/18	10.6
GCS 16	2291	17 <sup>h</sup> 45 <sup>m</sup> 55 <sup>s</sup>	−29° 12′ 34″	2001/07/18	10.6
GCS 17	2293	17 <sup>h</sup> 45 <sup>m</sup> 09 <sup>s</sup>	−29° 06′ 28″	2001/07/19	11.1
GCS 20	2267	17 <sup>h</sup> 44 <sup>m</sup> 41 <sup>s</sup>	−29° 16′ 27″	2001/07/19	11.5
SGR A*	2943	17 <sup>h</sup> 45 <sup>m</sup> 41 <sup>s</sup>	−29° 00′ 15″	2002/05/22	38.0
SGR A*	3663	17 <sup>h</sup> 45 <sup>m</sup> 41 <sup>s</sup>	−29° 00′ 15″	2002/05/24	38.0
SGR A*	3392	17 <sup>h</sup> 45 <sup>m</sup> 41 <sup>s</sup>	−29° 00′ 15″	2002/05/27	166.7
SGR A*	3393	17 <sup>h</sup> 45 <sup>m</sup> 41 <sup>s</sup>	−29° 00′ 15″	2002/05/30	158.0
SGR A*	3665	17 <sup>h</sup> 45 <sup>m</sup> 41 <sup>s</sup>	−29° 00′ 15″	2002/06/03	89.9

<sup>a</sup> The net exposure time after filtering - EPIC MOS1/MOS2/pn in the case of *XMM-Newton* and ACIS-I in the case of *Chandra*.

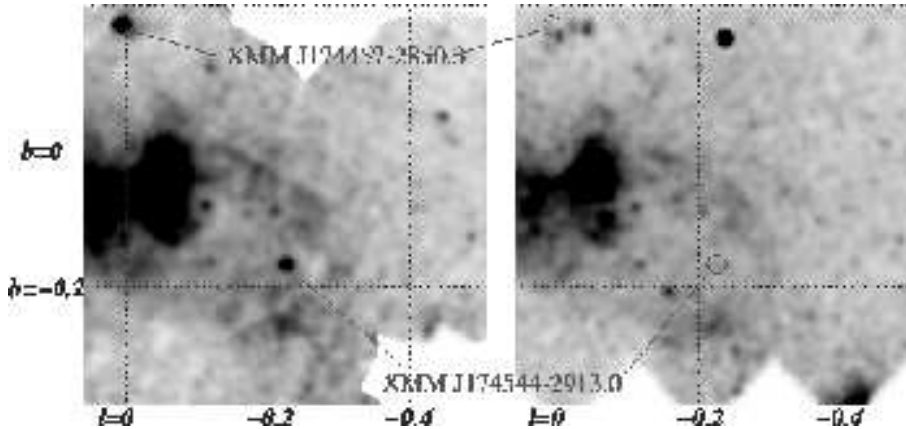


**Figure 1.** Sub-regions from the *XMM-Newton*/MOS1+2 (*left panel*) and *Chandra*/ACIS (*right panel*) mosaiced images of the Galactic Centre Region. The respective energy bands are 2–9 keV and 1–8 keV. Both images are background subtracted as well as vignetting and exposure corrected and have been smoothed with a circular Gaussian mask with  $\sigma = 20''$ . The grey-scaling is set such that regions of extended emission appear the same in the two images. The two transient sources which are the focus of the current paper are indicated. The bright extended feature on the eastern edge of the field of view is the Sgr A region (e.g., Maeda et al. 2002; Sakano et al. 2004b).

the F-test<sup>†</sup>. The line equivalent width was found to be 180 eV with a 90% confidence interval of 40–320 eV (90% confidence intervals assuming one interesting parameter are used throughout this paper). The best-fitting model and parameters including the line are shown in Fig. 3 and Table 3, respectively. On the basis of the line energy measurement, the line is very likely to be the 6.7-keV K-line from helium-like

<sup>†</sup> The F-test may underestimate the significance in this case (Prottasov et al. 2002). However the result here that the line is significant would be unchanged.

iron. To check the contribution of the detector and diffuse background to this line we tried a 50% larger normalisation for the background data; the result was that the significance and the intensity of the line were hardly affected. The observed 2–10 keV flux of  $4.5 \times 10^{-12} \text{ erg s}^{-1} \text{ cm}^{-2}$  converts to an absorption-corrected luminosity of  $4.5 \times 10^{34} \text{ erg s}^{-1}$ , assuming a distance of 8.0 kpc (Reid 1993).

A remarkable feature of the source spectrum is the apparent hardness of the continuum. In effect, this excludes a thermal bremsstrahlung model – an actual fit gave a 90% lower limit for the temperature of such a component to be 35 keV.

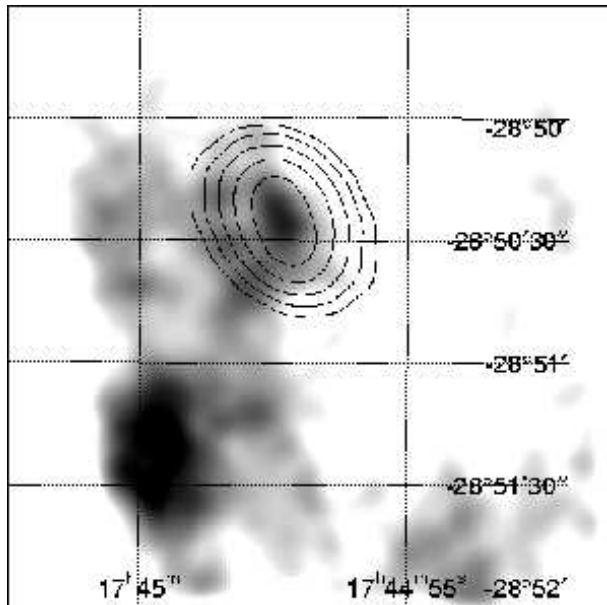


**Figure 2.** Chandra 2–8 keV image of the XMM J174457–2850.3 region based on the combined 2002 data. The contours represent the point spread function (PSF) at this off-axis location. Both the image and the PSF are smoothed with a Gaussian filter with  $\sigma = 3''$ . The grey-scale and contour levels are logarithmically spaced.

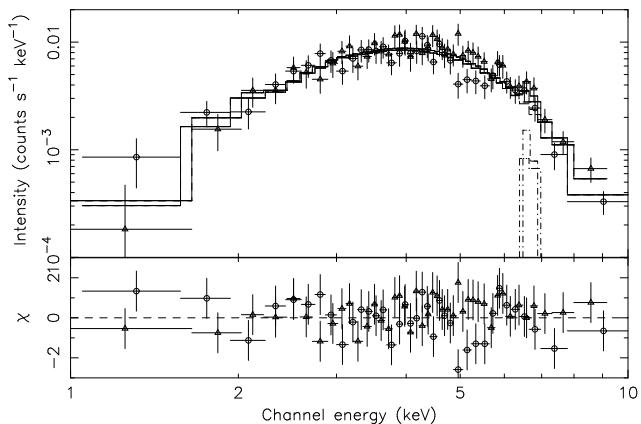


**Figure 3.** EPIC MOS spectra of XMM J174457–2850.3 from the September 2001 (GC6) observation. The open circles and triangles represent MOS1 and MOS2 data, respectively. The best-fitting model is shown as a histogram. The lower panel shows the residuals to the best-fitting model.

We have also analysed the ACIS-S spectrum of XMM J174457–2850.3 as obtained from the co-added *Chandra* data of 2002 May/June. In order to obtain the maximum signal-to-noise ratio and to minimize the uncertainty due to possible spatial variation of the diffuse component (see Fig. 2), we chose a relatively small region for the accumulation of the source spectrum, namely an elliptical region encompassing the central part of the PSF, with semi-axes of  $10''$  and  $5''$ . We then collected the background spectrum from a region east of the source position, where some diffuse emission extending from the source region is seen.

The background-subtracted *Chandra* spectrum was modelled with a power-law continuum with the low-energy

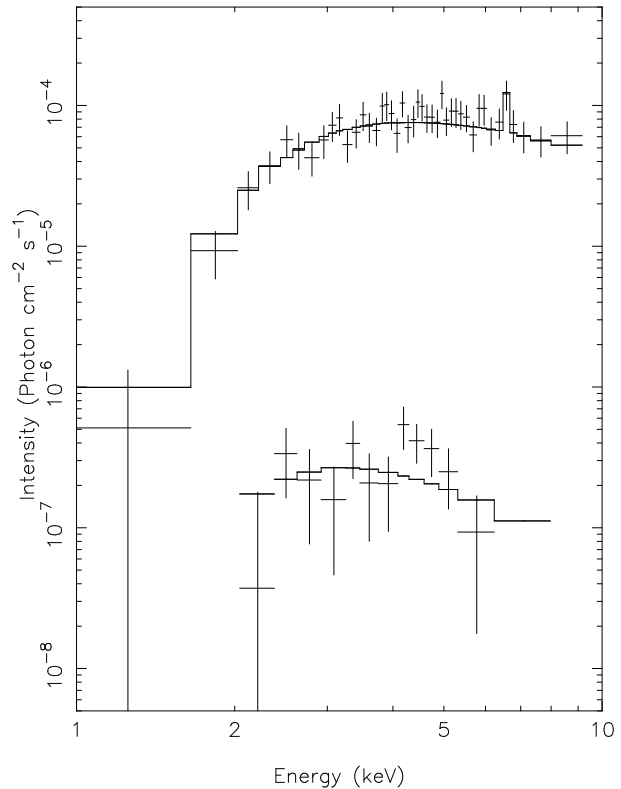


**Figure 4.** Unfolded X-ray spectra of XMM J174457–2850.3. The upper and lower data are taken with *XMM-Newton* (MOS2) in 2001 and with *Chandra* (ACIS-I) in 2002, respectively.

absorption fixed at the value obtained from the *XMM-Newton* high-state measurement. The derived best-fitting photon index was 1.9 (1.1–2.8) (Table 3). In this case the addition of an iron line at 6.7 keV did not improve the fit with a 90% upper limit on the equivalent width of such a line determined to be 760 eV. The observed 2–10 keV flux is  $1.0 \times 10^{-14} \text{ erg s}^{-1} \text{ cm}^{-2}$ , corresponding to an absorption-corrected luminosity of  $1.2 \times 10^{32} \text{ erg s}^{-1}$ . Fig. 4 compares the unfolded spectra of XMM J174457–2850.3 in the high and low states.

### 3.2 XMM J174544–2913.0

XMM J174544–2913.0 is in the field of view for 5 of the observations listed in Table 1. Table 2 summarises, in chronological order, the X-ray flux measurements at the source position. The source was detected only in the first observation (September 2000) and was at least two orders of magnitude fainter some 10 months later.

Within the *XMM-Newton* GC10 observation the emission from the source was found to be rather stable. For example fitting the light curve with a constant emission model (after background subtraction) for a binning of 32 s and 64 s gives acceptable  $\chi^2$  values. A search for pulsations using a FFT algorithm provided no evidence for a significant periodic signal.

We extracted MOS spectra from the GC10 observation using a  $52''$  radius source cell centred on XMM J174544–2913.0. Corresponding background spectra were taken from a concentric annulus with inner and outer radii

**Table 2.** The measured X-ray flux and derived X-ray luminosity of the two sources.

Date	Satellite	Field	XMM J174457–2850.3		XMM J174544–2913.0	
			$F_X^a$	$L_X^b$	$F_X^a$	$L_X^b$
2000/09/24	<i>XMM</i>	GC10	—	—	37	5
2001/04/01	<i>XMM</i>	GRO J1744–28	<1.6	<0.2	—	—
2001/07/18	<i>Chandra</i>	GCS 12	$1.2 \pm 0.2$	$0.12 \pm 0.02$	—	—
2001/07/18	<i>Chandra</i>	GCS 14	<0.5	<0.05	—	—
2001/07/18	<i>Chandra</i>	GCS 15	<3.1	<0.3	—	—
2001/07/18	<i>Chandra</i>	GCS 16	—	—	<0.3 <sup>c</sup>	<0.04 <sup>c</sup>
2001/07/19	<i>Chandra</i>	GCS 17	—	—	<0.4	<0.05
2001/07/19	<i>Chandra</i>	GCS 20	—	—	<0.8	<0.11
2001/09/04	<i>XMM</i>	GC6	45	5	<1.7	<0.2
2002/05/22	<i>Chandra</i>	SGR A*	< 0.23	< 0.027	—	—
2002/05/24	<i>Chandra</i>	SGR A*	< 0.20	< 0.023	—	—
2002/05/27	<i>Chandra</i>	SGR A*	$0.13 \pm 0.024$	$0.015 \pm 0.003$	—	—
2002/05/30	<i>Chandra</i>	SGR A*	< 0.17	< 0.019	—	—
2002/06/03	<i>Chandra</i>	SGR A*	< 0.21	< 0.025	—	—
2001/07/18–19	<i>Chandra</i>	GCS 16+17	—	—	<0.2	<0.03
2002/05/22–06/04	<i>Chandra</i>	SGR A*	$0.10 \pm 0.014$	$0.012 \pm 0.0016$	—	—

<sup>a</sup> The observed 2–10 keV flux in units of  $10^{-13} \text{ erg s}^{-1} \text{ cm}^{-2}$ .

<sup>b</sup> The 2–10 keV absorption-corrected luminosity in units of  $10^{34} \text{ erg s}^{-1}$ .

<sup>c</sup> The position of XMM J174544–2913.0 is close to a chip gap ( $\sim 15$  arcsec). If the true source position is located closer to the chip gap than our current estimate, these upper limits may have to be increased by up to 50%.

**Table 3.** The best-fitting spectral parameters plus 90% confidence intervals for the two sources.

	Obs.	$N_H^a$	$\Gamma$	$F_{6.7}^b$	$E_{6.7}^c$	$F_X^d$	$\chi^2/\text{dof}$
XMM J174457–2850.3	GC6	5.86 (4.95–7.12)	0.98 (0.73–1.31)	0.12 (0.03–0.22)	6.65 (6.46–6.74)	4.5	58.9/75
	SGR A*	5.86 (fixed)	1.92 (1.07–2.81)	—	—	0.010	14.9/11
XMM J174544–2913.0	GC10	12.4 (10.7–14.2)	2.00 (1.73–2.13)	1.14 (0.91–1.35)	6.68 (6.66–6.70)	3.7	44.8/41

<sup>a</sup> Hydrogen column density ( $10^{22} \text{ H cm}^{-2}$ ).

<sup>b</sup> 6.7 keV line flux ( $10^{-4} \text{ ph s}^{-1} \text{ cm}^{-2}$ )

<sup>c</sup> Line-centre energy (keV)

<sup>d</sup> Observed 2–10 keV flux ( $10^{-12} \text{ erg s}^{-1} \text{ cm}^{-2}$ ).

of  $52''$  and  $80''$ , respectively. The source was outside of the field of view of the pn camera in this observation.

Fig. 5 shows the EPIC MOS1 and MOS2 spectra after background subtraction. A line feature is very prominent between 6–7 keV. We fitted the two MOS spectra simultaneously with a model comprising a power-law continuum plus a narrow Gaussian line. This simple model provides a good match to the observed spectrum with a  $\chi^2(\text{dof})$  of 44.8 (41). The best-fitting parameter values are summarised in Table 3 and Fig. 5 shows the corresponding best-fitting model and the fitting residuals. The measured line-centre energy, 6.68 (6.66–6.70) keV, is consistent with the dominant transition being the 6.7-keV  $K\alpha$  line from helium-like iron. The line equivalent width is remarkably high, namely 2.4 (1.9–2.8) keV. The 2–10 keV luminosity is calculated to be  $5 \times 10^{34} \text{ erg s}^{-1}$ , assuming a distance of 8.0 kpc.

We also tried a thin-thermal plasma model, allowing the iron abundance to vary but fixing all the rest of the abun-

dances at the solar values (Anders & Grevesse 1989). The fitting result is found to be acceptable ( $\chi^2/\text{dof}=47.5/42$ ). The best-fitting temperature and iron abundance are 3.9 (2.6–5.3) keV and 3.1 (1.9–5.1) solar, respectively.

## 4 DISCUSSION

Both transient sources have X-ray spectra characterised by substantial soft X-ray absorption, corresponding to  $N_H = 6 \times 10^{22} \text{ H cm}^{-2}$  in the case of XMM J174457–2850.3 and twice this value for XMM J174544–2913.0. Given the measured range of column densities associated with Galactic Centre features and sources (Sakano et al. 1999; Sakano 2000), it is perfectly plausible that both sources are located in the vicinity of the Galactic Centre. Thus, the assumption of a distance of 8.0 kpc (Reid 1993) from which we infer peak observed X-ray luminosities of  $5 \times 10^{34} \text{ erg s}^{-1}$  would seem to

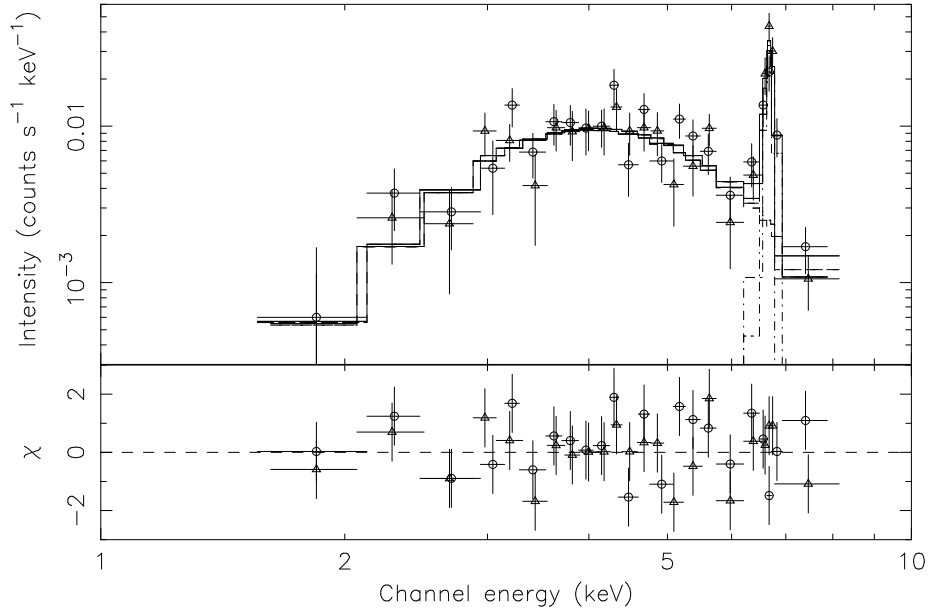


**Figure 5.** XMM EPIC spectra of XMM J174544–2913.0 from the September 2000 (GC10) observation. The open circles and triangles represent MOS1 and MOS2 data, respectively. The best-fitting model for each dataset is shown as a histogram.

be a reasonable one. For both sources the lowest observed “quiescent” luminosity is at least two orders of magnitude below the peak level.

#### 4.1 Classification of XMM J174457–2850.3

XMM J174457–2850.3 has a very flat X-ray spectrum with a relatively weak He-like iron line (equivalent width of  $\sim 200$  eV). This spectral description matches two source classes: cataclysmic variables (CVs) in which the magnetic field of the white dwarf star controls the accretion flow (i.e., polars and intermediate polars, see Ezuka & Ishida 1999) or high-mass X-ray binaries (HMXBs) in which a neutron star accretes from the wind of a young massive companion. The inferred X-ray luminosity in the high state of  $5 \times 10^{34} \text{ erg s}^{-1}$  presents a problem for the former interpretation since this is a factor  $\sim 10$  times higher than is observed in even the brightest magnetic CVs (Verbunt et al. 1997; Ezuka & Ishida 1999; Pooley et al. 2002; Baskill, Wheatley & Osborne 2004). HMXBs are more typically seen in outburst with luminosities of  $L_X > 10^{36} \text{ erg s}^{-1}$  but this apparent high luminosity preference could well be a selection effect (Pfahl, Rappaport & Podsiadlowski 2002). Similarly the quiescent luminosity of  $1 \times 10^{32} \text{ erg s}^{-1}$  is lower than the observed lower limit for most HMXBs ( $> 5 \times 10^{32} \text{ erg s}^{-1}$ ; Munro et al. 2003a). Modulation of the X-ray light curve arising from the spin period of a wind-accreting neutron star can be of relatively large amplitude (5%–50%) (see Munro et al. 2003b). However the search for an underlying coherent periodicity in XMM J174457–2850.3 is limited by both the statistics and exposure even when the source was in its high state. If the equivocal period of 5.2521 s could be shown to be a genuine periodicity, then this would lend support to the HMXB scenario. Also, if the weak diffuse emission seen at and near the location of XMM J174457–2850.3 could be associated with

a star forming region, then the HMXB scenario would gain further credence.

#### 4.2 Classification of XMM J174544–2913.0

The most interesting spectral property of this source is its extremely strong iron line (equivalent width of  $\sim 2.4$  keV). In general, low-mass X-ray binaries (LMXBs) show little evidence for line emission, whereas HMXBs sometimes show significant Fe lines, presumably emitted in the region of the stellar wind of the companion star. However an equivalent width of over 1 keV is not normally seen in such circumstances. In addition, the quiescent X-ray luminosity of XMM J174544–2913.0 is unusually low for a HMXB (e.g., Munro et al. 2003). Active stellar coronal sources such as RS-CVn systems, Wolf-Rayet (WR) stars and Young Stellar Objects (YSO) usually have much lower luminosities ( $\leq 10^{32.5} \text{ erg s}^{-1}$  at peak) and hence are not likely candidates, although they often show an iron line and significant flares. Massive WR-OB star binaries may have 2–10 keV X-ray luminosities up to  $10^{35} \text{ erg s}^{-1}$ , presumably due to wind-wind collisions (Portegies Zwart, Pooley & Lewin 2002). In addition they often show a strong iron K-line with an equivalent width of  $\sim 1$  keV. However, here the problem is the factor 100 change in luminosity – for example, an extensive study covering the different orbital phases shows the variability in the hard X-ray component in such systems is at most a factor of three (Maeda et al. 1999). A background active galaxy, seen through the Galaxy, might conceivably be a candidate but again it is very difficult to match the observations with any known class of object. For example, in Seyfert I nuclei the measured 6.7-keV line equivalent width is invariably less than a few hundred eV (e.g., Nandra & Pounds 1994; Reeves & Turner 2000), whereas the extreme variability excludes an obscured Seyfert II nucleus (e.g., Koyama et al. 1989) as a potential counterpart.

The nature of XMM J174544–2913.0 is remarkably similar to AX J1842.8–0423, which was discovered in an *ASCA* survey of the Scutum arm region in 1996 (Terada et al. 1999). Terada et al. (1999) found that AX J1842.8–0423 has a strong iron line at 6.8 keV with an equivalent width of  $\sim 4$  keV. The spectrum is well approximated with a thin-thermal plasma model with a temperature of  $kT \sim 4$  keV and heavy-metal abundance of  $\sim 3$  solar. AX J1842.8–0423 also showed transient behaviour on a time-scale of less than half a year. In addition there are two other sources which have an extremely strong iron line: AX J2315–592 (CP Tuc; Miskaki et al. 1996) and RX J1802.1+1804 (V884 Her; Ishida et al. 1998). Both of the latter sources have been identified as polars (i.e. AM Her type CVs).

Terada et al. (1999, 2001) concluded that the three sources above are probably close binaries involving a magnetised white dwarf viewed from a pole-on inclination. In fact, although many CVs show an iron line, the equivalent width of such features is typically a couple of hundred eV or less, or the iron abundance is generally sub-solar (e.g., Ezuka & Ishida 1999). However, Terada et al. (1999, 2001) argued that the observed strong iron line is interpreted as due to line-photon collimation in the accretion column of the white dwarf, as a result of resonance scattering of line photons, which may occur in the case of a pole-on inclination.

Table 4 summarises the properties of the three sources considered by Terada et al. in comparison to those of XMM J174544–2913.0. The extremely strong iron line may be explained with the model of Terada et al. However its high luminosity of  $\sim 10^{34}$  erg  $s^{-1}$  still remains a major problem as discussed in the previous section (§4.1).

Given the uncertainty pertaining to the CV scenario, what other possibilities are there? It is plausible that this source represents a new type of neutron star binary which, for some reason, is relatively efficient at producing strong iron lines. In this case, the transient nature and high luminosity would be easily explained. Alternatively, a massive WR-OB star binary in an extremely eccentric orbit might conceivably give rise to transient-like activity. Clearly, it remains to be demonstrated whether XMM J174544–2913.0 corresponds to a known class of source in an extreme configuration or to an entirely new class of object.

### 4.3 The origin of the Galactic Centre 6.7-keV line emission

Recent deep observations with *Chandra* have shown that the bulk of the hard X-ray emission associated with the inner Galactic Plane is not due to the summed emission of faint Galactic sources, at least down to a limiting source luminosity of  $L_X \approx 10^{31}$  erg  $s^{-1}$  (Ebisawa et al. 2001). The demonstration that this feature, known as the Galactic Ridge (e.g., Worrall et al. 1982; Warwick et al. 1985; Koyama et al. 1986; Yamauchi & Koyama 1993; Kaneda et al. 1997; Valinia & Marshall 1998), is truly diffuse in origin represents a major step forward. However, our understanding of the processes that produce both the hard continuum and the associated line emission from highly ionized ions, most notably helium-like iron at 6.7-keV, remains incomplete (e.g., Tanaka et al. 2000; Tanaka 2002; Valinia et al. 2000). Interestingly the hard X-ray emission observed

from the Galactic Centre Region has very similar spectral characteristics to that of the Galactic Ridge (Koyama et al. 1996; Kaneda et al. 1997; Tanaka et al. 2000; Tanaka 2002) except for its much higher surface brightness in the Galactic Centre Region.

The high concentration of point sources observed within  $9'$  of the Galactic Centre by *Chandra* (Muno et al. 2003a) suggests the possibility that, at least in this region, point sources may contribute significantly to the total observed emission. Particularly intriguing in this respect is the fact that the integrated spectrum of faint resolved sources is extremely hard ( $\Gamma \approx 0.8$ ) with a strong He-like iron line (equivalent width of  $\sim 400$  eV) (Muno et al. 2004b). However, investigation of the *Chandra*  $\log N$ - $\log S$  curve for resolved X-ray sources shows that such sources account for only  $\sim 10\%$  of the total 2–8 keV emission (Muno et al. 2004a). If unresolved sources make up the deficit, the requirement is for a total of  $2 \times 10^5$  sources within 20 pc ( $9'$ ) of Sgr A\* with a typical luminosity  $L_X \sim 10^{30}$  erg  $s^{-1}$ . In fact the implied source number density substantially exceeds the estimated  $10^4$  CVs in the region and, together with the additional luminosity and spectral constraints, matches no known population of sources (Muno et al. 2004a).

Our observation of XMM J174544–2913.0 suggests one further possibility. This source has very strong 6.7-keV iron line emission and in fact the line equivalent width of  $\sim 2.4$  keV is roughly 6 times that of the average faint source resolved by *Chandra* to a limiting luminosity of  $\sim 10^{31}$  erg  $s^{-1}$ . Might therefore similar sources explain all or part of the 6.7-keV line emission without necessarily also accounting for the bulk of the hard continuum?

We estimate from unpublished *XMM-Newton* data that the total 6.7-keV iron-line flux from the region within  $9'$  of the Galactic Centre is  $\sim 7 \times 10^{-4}$  photon  $s^{-1}$   $cm^{-2}$ , excluding the contribution of the Sgr A East SNR (Maeda et al. 2002; Sakano et al. 2004a, b). The 6.7-keV line flux of XMM J174544–2913.0 in its high state is  $1.1 \times 10^{-4}$  photon  $s^{-1}$   $cm^{-2}$  (Table 3). However, no other similar source (in terms of the line properties) is seen at the same flux level in the *XMM-Newton* Galactic Centre Survey. Also since we have established that the source is a transient, it is clear the presence of relatively large numbers of such sources in quiescence is of principle concern. If we assume that these transient sources keep their spectral shape, including the large equivalent width of their 6.7-keV line, in their quiescent state, then the number of XMM J174544–2913.0-type sources required to explain the whole 6.7-keV line intensity of the central region is  $\sim 30000 L_{31}^{-1}$ , where  $L_{31}$  is the typical quiescent luminosity in units of  $10^{31}$  erg  $s^{-1}$ . As expected the integrated emission of such sources would account for only  $\sim 15\%$  of the 2–8 keV continuum and might be a poor match to the slope of the observed spectrum (this is uncertain since XMM J174544–2913.0 has a rather soft continuum form but also a substantial column density).

Unfortunately this scenario looks barely viable. If  $L_{31} > 10$  then such sources should be appearing in large numbers (with prominent 6.7 keV lines) in the *Chandra* surveys. At  $L_{31} \approx 1$  such sources should again be appearing as faint resolved *Chandra* sources, yet the measured 6.7-keV line equivalent width of the integrated resolved-source spectrum limits their contribution to  $\sim 15\%$ . Conversely, if the quiescent state of such transients is at fainter levels (i.e.  $L_{31} < 0.3$ ),

**Table 4.** The spectral parameters for four sources with strong iron 6.7-keV emission.

Name	$N_{\text{H}}$ ( $10^{22} \text{H cm}^{-2}$ )	$kT$ (keV)	$E_{6.7}^a$ (keV)	$\text{EW}_{6.7}^a$ (keV)	$Z_{\text{Fe}}^b$	$L_{\text{X}}^c$ ( $\text{erg s}^{-1}$ )	ID <sup>d</sup>	Tr? <sup>e</sup>	Ref.
AX J2315–592	<0.07	$16.5_{-3.1}^{+3.0}$	$6.84_{-0.09}^{+0.13}$	$0.9_{-0.2}^{+0.3}$	$1.93_{-0.43}^{+0.56}$	$1 \times 10^{32} d_{0.2}^2$	Yes	No	1,2,3
RX J1802.1+1804 <sup>f</sup>	~0.01	~0.9	$6.55_{-0.08}^{+0.09}$	$4.0_{-1.7}^{+1.7}$	1.3 – 12	$6 \times 10^{29} d_{0.1}^2$	Yes	No	4,5
AX J1842.8–0423	$3.9_{-1.1}^{+1.1}$	$5.1_{-1.9}^{+5.0}$	$6.78_{-0.13}^{+0.10}$	$4.0_{-0.5}^{+1.0}$	$3.0_{-0.9}^{+4.3}$	$1.6 \times 10^{34} d_5^2$	No	Yes	6
XMM J174544–2913.0	$12.4_{-1.7}^{+1.8}$	$3.9_{-1.3}^{+1.4}$	$6.68_{-0.02}^{+0.02}$	$2.4_{-0.5}^{+0.4}$	$3.1_{-1.2}^{+2.0}$	$5 \times 10^{34} d_8^2$	No	Yes	7

References – 1: Misaki et al. 1996; 2: Thomas & Reinsch 1996; 3: Ramsay et al. 1999; 4: Ishida et al. 1998; 5: Greiner et al. 1998; 6: Terada et al. 1999; 7: this work.

<sup>a</sup> Centre energy ( $E_{6.7}$ ) and equivalent width ( $\text{EW}_{6.7}$ ) of the 6.7-keV line.

<sup>b</sup> Iron abundance relative to the solar abundance ratio.

<sup>c</sup> The 2–10 keV luminosity (in the high state if the source shows the transient activity). *d* indicates the distance; e.g.,  $d_8$  is the distance in units of 8 kpc.

<sup>d</sup> Are there any optical/IR identifications?

<sup>e</sup> Has X-ray transient activity ever been observed?

<sup>f</sup> Results for a single absorption and single temperature model.

then the required source density becomes excessive, particularly if there is an association with CVs.

## 5 CONCLUSION

We have discovered two X-ray transient sources, XMM J174457–2850.3 and XMM J174544–2913.0, in the Galactic Centre Region with *XMM-Newton*. The observations of *XMM-Newton* and *Chandra* revealed that the flux of the two sources changed by more than two orders of magnitude in less than a year. Their heavy absorption in the high state gives a strong indication that both the sources are located in the Galactic Centre Region. The peak fluxes of both the sources are  $\sim 4 \times 10^{-12} \text{erg s}^{-1} \text{cm}^{-2}$ , equivalent to an X-ray luminosity of  $\sim 5 \times 10^{34} \text{erg s}^{-1}$ , suggesting a new transient population with a peak luminosity up to three orders of magnitude below that typical of X-ray transients in our Galaxy. XMM J174544–2913.0 shows a strong emission line at 6.7 keV, presumably a K-line from helium-like iron, with an equivalent width of  $\sim 2.4$  keV. The nature is very similar to AX J1842.8–0423. However, no known class of sources can well explain all their characteristics. XMM J174457–2850.3 has a very flat spectrum ( $\Gamma \sim 1.0$ ) with a possible weak line from He-like iron. It is the most likely a neutron star or black hole binary, possibly with a high-mass companion.

## ACKNOWLEDGMENTS

The authors would like to express their thanks to all those who have contributed to the successful development and operation of *XMM-Newton*. We are grateful to J. Tedds, D. Baskill and the anonymous referee for their valuable comments. In addition we should like to acknowledge the help of many colleagues at Leicester, especially R. Saxton, S. Sembay, I. Stewart and M.J.L. Turner, on matters relating to the EPIC calibration and the use of the SAS.

## REFERENCES

- Anders E. & Grevesse N., 1989, *Geochimica et Cosmochimica Acta*, 53, 197
- Baganoff F.K. et al., 2001, *Nature*, 413, 45
- Baganoff F.K. et al., 2003, *ApJ*, 591, 891
- Baskill D.S., Wheatley P.J., Osborne J.P., 2004, *MNRAS*, submitted
- Ebisawa K., Maeda Y., Kaneda H., Yamauchi S., 2001, *Science*, 293, 1633
- Ezuka H., Ishida M., 1999, *ApJS*, 120, 277
- Goldwurm A. et al., 2001, *ApJ*, 584, 751
- Greiner J., Remillard R.A., Motch C., 1998, *A&A*, 336, 191
- Ishida M., Greiner J., Remillard R.A., Motch C., 1998, *A&A*, 336, 200
- Kaneda H., Makishima K., Yamauchi S., Koyama K., Matsuzaki K., Yamasaki N.Y., 1997, *ApJ*, 491, 638
- Koyama K., Makishima K., Tanaka Y., Tsunemi H., 1986, *PASJ*, 38, 121
- Koyama K., Inoue H., Tanaka Y., Awaki H., Takano S., Ohashi T., Matsuoka M., 1989, *PASJ*, 41, 731
- Koyama K., Maeda Y., Sonobe T., Takeshima T., Tanaka Y., Yamauchi S., 1996, *PASJ*, 48, 249
- Maeda Y., Koyama K., Yokogawa J., Skinner S., 1999, *ApJ*, 510, 967
- Maeda Y. et al., 2002, *ApJ*, 570, 671
- Misaki K., Terashima Y., Kamata Y., Ishida M., Kunieda H., Tawara Y., 1996, *ApJ*, 470, L53
- Muno M.P. et al., 2003a, *ApJ*, 589, 225
- Muno M.P. Baganoff F.K., Bautz M.W., Brandt W.N., Garmire G.P., Ricker G.R., 2003b, *ApJ*, 599, 465
- Muno M.P. et al., 2004a, *ApJ*, in press (*astro-ph/0402087*)
- Muno M.P. et al., 2004b, *ApJ*, in press (*astro-ph/0403463*)
- Nandra K., Pounds K.A., 1994, *MNRAS*, 268, 405
- Pfahl E., Rappaport S., Podsiadlowski P., 2002, *ApJ*, 571, L37
- Pooley D. et al., 2002, *ApJ*, 569, 405
- Porquet D. et al., 2003, *A&A*, 407, 17
- Portegies Zwart S.F., Pooley D., Lewin W.H.G., 2002, *ApJ*, 574, 762
- Protassov R., van Dyk D.A., Connors A., Kashyap V.L., Siemiginowska A., 2002, *ApJ*, 571, 545
- Ramsay G., Potter S.B., Buckley D.A.H., Wheatley P.J., 1999, *MNRAS*, 306, 809
- Reeves J.N., Turner M.J.L., 2000, *MNRAS*, 316, 234
- Reid M.J., 1993, *ARA&A*, 31, 345



- Sakano M., Koyama K., Nishiuchi M., Yokogawa J., Maeda Y., 1999, *Advances in Space Research*, 23(5/6), 969
- Sakano M., 2000, PhD thesis, Kyoto University
- Sakano M., Koyama K., Murakami H., Maeda Y., Yamauchi S., 2002, *ApJS*, 138, 19
- Sakano M., Warwick R.S., Decourchelle A., 2003, in Ohashi T., Yamasaki N.Y., eds, *Proc. Workshop on Galaxies and Clusters of Galaxies*, JSPS, Tokyo, p.9 (astro-ph/0212464)
- Sakano M., Warwick R.S., Decourchelle A., 2004a, *Advances in Space Research*, 33, 403
- Sakano M., Warwick R.S., Decourchelle A., Predehl P., 2004b, *MNRAS*, 350, 129
- Sakano M., Warwick R.S., Hands A., Decourchelle A., 2004c, *Memorie della Società Astronomica Italiana*, 350, 129
- Sidoli L., Mereghetti S., Israel G.L., Chiappetti L., Treves A., Orlandini M., 1999, *ApJ*, 525, 215
- Soker N., Lasota J.-P., 2004, *A&A*, 422, 1039
- Strüder L. et al., 2001, *A&A*, 365, L18
- Tanaka Y., Koyama K., Maeda Y., Sonobe T., 2000, *PASJ*, 52, L25
- Tanaka Y., 2002, *A&A*, 382, 1052
- Terada Y., Kaneda H., Makishima K., Ishida M., Matsuzaki K., Nagase F., Kotani T., 1999, *PASJ*, 51, 39
- Terada Y., Ishida M., Makishima K., Imanari T., Fujimoto R., Matsuzaki K., Kaneda H., 2001, *MNRAS*, 328, 112
- Thomas H.-C., Reinsch K., 1996, *A&A*, 315, L1
- Turner M.J.L. et al., 2001, *A&A*, 365, L27
- Valinia A., Marshall F.E., 1998, *ApJ*, 505, 134
- Valinia A., Tatischeff V., Arnaud K., Ebisawa K., Ramaty R., 2000, *ApJ*, 543, 733
- Verbunt F., Bunk W.H., Ritter H., Pfeffermann E., 1997, *A&A*, 327, 602
- Wang Q.D., Gotthelf E.V., Lang C.C., 2002, *Nature*, 415, 148
- Warwick R.S., Turner M.J.L., Watson M.G., Willingale R., 1985, *Nature*, 317, 218
- Warwick R.S., 2002, *Proc. New Visions of the X-ray Universe in the XMM-Newton and Chandra era.*, in press (astro-ph/0203333)
- Worrall D.M., Marshall F.E., Boldt E.A., Swank J.H., 1982, *ApJ*, 255, 111
- Yamauchi S., Koyama K., 1993, *ApJ*, 404, 620